Drug Delivery

http://informahealthcare.com/drd
ISSN: 1071-7544 (print), 1521-0464 (electronic)

Drug Deliv, 2016; 23(8): 3055–3062
 DOI: 10.3109/10717544.2016.1145306

Taylor & Francis
Taylor & Francis Group

RESEARCH ARTICLE

Effect of microemulsion formulation on biodistribution of ^{99m}Tc-Aprotinin in acute pancreatitis models induced rats

Derya İlem-Özdemir[1], Neslihan Üstündağ-Okur[2], Zeynep Ay Şenyiğit[3], Nevin Oruç[4], Makbule Aşıkoğlu[1], Ömer Özütemiz[4], and H. Yeşim Karasulu[3]

[1]Department of Radiopharmacy, Faculty of Pharmacy, Ege University, Izmir, Turkey, [2]Department of Pharmaceutical Technology, School of Pharmacy, Istanbul Medipol University, Istanbul, Turkey, [3]Department of Pharmaceutical Technology, Faculty of Pharmacy, and [4]Department of Gastroenterology, Faculty of Medicine, Ege University, Izmir, Turkey

Abstract

Background: Aprotinin is a monomeric globular polypeptide, which derived from bovine lung tissue and theoretically attractive molecule in ameliorating the effects of acute pancreatitis. Acute pancreatitis is an inflammatory condition of the pancreas that is painful and at times deadly. Over the following two decades Aprotinin therapeutic potential on pancreatitis is proven experimentally, its clinical therapeutic success is limited due to low targeting to pancreas.

Objective: The aim of this study was to evaluate the biodistribution of Technetium-99m (^{99m}Tc)-Aprotinin solution (^{99m}Tc-Aprotinin-S) and ^{99m}Tc-Aprotinin loaded microemulsion, which was prepared for the aim of treatment for acute pancreatitis.

Method: Aprotinin was radiolabeled with ^{99m}Tc. Radiochemical purity was determined with radioactive thin layer chromatography studies. ^{99m}Tc-Aprotinin-S and ^{99m}Tc-Aprotinin loaded microemulsion (^{99m}Tc-Aprotinin-M) was administered to acute edematous, severe necrotizing pancreatitis and air pouch model induced rats. Tissue distribution of Aprotinin was investigated with gamma scintigraphy and biodistribution studies.

Results: Aprotinin was radiolabeled by ^{99m}Tc with high radiochemical purity (95.430 ± 0.946%). The complex was found to be stable at room temperature up to 6 h. Animal studies have shown that similar to that of other small proteins Aprotinin is accumulated primarily in the kidney. The scintigraphy and biodistribution studies showed that, while i.v. administration of ^{99m}Tc-Aprotinin-S distributed mostly in kidneys and bladder, ^{99m}Tc-Aprotinin-M, with droplet size of 64.550 ± 3.217 nm, has high uptake in liver, spleen and pancreas.

Conclusion: This might be concluding that microemulsions may be suggested as promising formulations for selectively targeting Aprotinin to pancreas inflammation.

Keywords

Aprotinin, biodistribution, microemulsion, pancreatitis, radiolabeled Aprotinin

History

Received 1 December 2015
Revised 15 January 2016
Accepted 19 January 2016

Introduction

Aprotinin is a monomeric globular polypeptide, which derived from bovine lung tissue. It is a 58 amino acid residue protein chain with three disulfide bonds, one α helix and two sheets, a structure and belongs to the Kunitz family of serine proteinase inhibitors. It inhibits human trypsin, plasmin, plasma and tissue kallikreins, by forming reversible stoichiometric enzyme-inhibitor complexes (Bode & Huber, 1992; Tiourina et al., 2003).

Inhibition of kallikrein results in prolongation of clotting times of the intrinsic cascade utilizing a positive feedback on the activation of factor XII, which is recognized in cardiac surgery (Hunt et al., 1992). Its efficacy in inhibiting plasmin is thought to account for its ability to reduce perioperative bleeding during open cardiac surgery where like other antifibrinolytics, it is of proven efficacy (Henry, 2007) (Kalkat et al., 2004).

The activation of the kallikrein–kinin system is thought to be one of the pathophysiologic mechanisms in acute pancreatitis. Since Aprotinin is a Kunitz protease inhibitor and has action particularly against trypsin, chymotrypsin and kallikrein potent proteinase inhibitors, it is theoretically attractive molecule in ameliorating the effects of acute pancreatitis (Bjerregaard et al., 2001; Smith et al., 2009).

Microemulsions are dispersed systems of water, oil and a surfactant/cosurfactant mixture. Importantly, from a formulation viewpoint, they form spontaneously and are thermodynamically stable (Graf et al., 2008; Üstündağ-Okur et al., 2015). Microemulsions are useful systems for parenteral applications because of their excellent thermodynamic stability, high solubilization capacity, low viscosity and ability to withstand sterilization techniques (Üstündağ-Okur et al., 2015). In addition, they are suitable dosage forms for peptide

Address for correspondence: Derya İlem-Özdemir, Department of Radiopharmacy, Faculty of Pharmacy, Ege University, Bornova, Izmir 35100, Turkey. Tel: +90 5334464026. Fax: +90 2323885258. Email: deryailem@gmail.com

and protein drug delivery. Microemulsion systems have also been claimed to improve storage stability of proteins (Ajit et al., 2007; Park et al., 2007).

Acute pancreatitis is an inflammatory condition of the pancreas that is painful and at times deadly. Despite the great advances in critical care medicine over the past 20 years, the mortality rate of acute pancreatitis has remained at about 10%. Diagnosis of pancreatic problems is often difficult and treatments are therefore delayed because the organ is relatively inaccessible (Edward, 1993). Over the following two decades Aprotinin therapeutic potential on pancreatitis is proven experimentally, its clinical therapeutic success is limited due to low targeting to pancreas (Karasulu et al., 2015).

Radionuclides are applied in the development of drugs as signal sources, which can be incorporated into formulation without any change of their characteristics. The main benefit of using radiolabeled compounds in drug development is to be sensitive and detectable for minimal amounts. The development of powerful radiotracers requires careful consideration in the selection of the radionuclide (Krauser, 2013). Choice of a suitable radionuclide for radiolabeling studies can be ascertained by considering factors such as the radiation energy, half-life, extent of particulate radiation, cost and availability. Technetium-99m (^{99m}Tc) is the most popular radionuclide with its versatile chemistry, near-ideal energy (140 keV), low radiation dose and short half-life (6 h) (Häfeli, 2002). ^{99m}Tc-Aprotinin has been used previously used for radionuclide kidney studies and amyloid detection and reported promising results in the demonstration of cardiac and pleura pulmonary amyloid (Wilding et al., 1991; Schaadt et al., 2003; Burke et al., 2007).

The aim of this study was to evaluate the biodistribution of ^{99m}Tc-Aprotinin solution (^{99m}Tc-Aprotinin-S) and ^{99m}Tc-Aprotinin loaded a microemulsion (^{99m}Tc-Aprotinin-M) formulation, which was prepared for the aim of the treatment for acute pancreatitis. For this purpose, Aprotinin was radiolabeled with ^{99m}Tc. Radiochemical purity was determined with radioactive thin layer chromatography (RTLC) studies. ^{99m}Tc-Aprotinin-S and ^{99m}Tc-Aprotinin-M were administered to acute edematous, severe necrotizing pancreatitis and air pouch model induced rats. Tissue distribution of Aprotinin was investigated with gamma scintigraphy and biodistribution studies.

Materials and methods

Materials

Aprotinin, Cremophor EL and stannous chloride ($SnCl_2{\cdot}2H_2O$) were purchased from Sigma (Germany) and oleic acid, isopropanol, sodium hydroxide and sodium dihydrogen phosphate were purchased from Merck (Germany). Glycine was purchased from Eczacibasi (Turkey). Saline was purchased from Adeka (Turkey) and water for injection was purchased from Sopharma (Turkey). ^{99m}Tc was eluted from the Molybdenum-99 (^{99}Mo)/^{99m}Tc-generator (Nuclear Medicine Department of Ege University). All chemicals and solvents were used without further purification. Dose Calibrator (Atomlab 100, Biodex Medical Systems, USA) was used for counting radioactive samples. Dual head gamma camera (Infinia General Electric, Germany) equipped with a low-energy high-resolution collimator was used for gamma scintigraphy studies. The Animal Ethics Committee of the Ege University gave approval for the animal experiments (Approval No. E.U(0).1344–249). Results are reported as mean ± standard error.

Radiolabeling studies

^{99m}Tc-Aprotinin was prepared using previously published method by Han et al. (2007) . Glycine phosphate alkaline buffer (pH 10.5) was prepared in advance by mixing 3.5% sodium dihydrogen phosphate in 1.0 M NaOH solution (1 ml), 1.5% glycine for irrigation (6 ml), saline (6 ml) and water for injection (9 ml) in a vial.

The reductant solution was freshly prepared before experiments by addition of sterile HCl (1 ml, 0.005 M) to 2 mg stannous chloride dehydrate ($SnCl_2$).

0.36 ml sterile Aprotinin (10 000 units/ml) was dissolved in glycine buffer (pH 10.5). To this stock solution, freshly prepared 0.1 ml $SnCl_2$ was added under an atmosphere of bubbling nitrogen. Radiolabeling was performed with ^{99m}Tc (37 MBq) in saline (0.1 ml) and solution was allowed to stand at room temperature for 20 min prior to radiochemical analyses. Radiochemical analysis was performed with RTLC studies.

RTLC procedure. Radiochemical purity of ^{99m}Tc-Aprotinin was analyzed by article and thin layer chromatography (TLC) studies. Albumin-impregnated instant TLC silica gel strips (ITLC-SG) were prepared by soaking in bovine serum albumin solution (5 mg/ml) for 30 min, and then the strips were rinsed with water, dried in air and then stored at 4 °C in a sealed container until required. The origin of each ITLC-SG strip was marked at 1 cm from one end of the strip. Whatman No. 3 papers and albumin-impregnated ITLC-SG strips were used as stationary phases, while acetone and ammonia/ethanol/water (A/E/W) (1/2/5) were mobile phases. Free ^{99m}Tc was determined by using acetone as the mobile phase. Reduced/hydrolyzed (R/H) ^{99m}Tc was determined by albumin impregnated strip, which developed in with ammonia/ethanol/water (A/E/W, 1/2/5).

Sample spot at the application point, strips were placed into two developing chambers containing acetone and A/E/W (1/2/5). After the solvent reached the end point (1 cm from the bottom), the strips were removed and allowed to dry. The radioactivity on plates was measured using a TLC scanner (Bioscan AR 2000, USA), and % radiochemical purity (RP) of ^{99m}Tc-Aprotinin was calculated from the following equation by subtracting from 100 the sum of measured impurities percentages.

$$\mathrm{RP}\,(\%) = 100 - \left(\text{Free } {}^{99m}\mathrm{Tc}\,(\%) + \frac{R}{H}\ {}^{99m}\mathrm{Tc}\,(\%)\right), \quad (1)$$

where Rp is the radiochemical purityand R/H ^{99m}Tc is the reduced/hydrolyzed ^{99m}Tc.

Preparation of ^{99m}Tc-Aprotinin-S

Two milligrams of Aprotinin included ^{99m}Tc-Aprotinin-S was prepared as prescribed above. Then, ^{99m}Tc-Aprotinin-S

filtered through a 0.22-mm membrane sterile filter (Minisart, Sartorius, Germany) into a sterile vial under laminar airflow Class II cabinet (EsCo Class 2, Selangor, Malaysia).

Preparation of ^{99m}Tc-Aprotinin-M

To formulate microemulsion systems pseudo-ternary phase diagrams were developed using titration of a series of oil and surfactant/cosurfactant (S/Cos) mixtures with 0.9% NaCl solution at ambient temperature ($25 \pm 2\,^{\circ}C$). Oil phase and the S/Cos mixture were then mixed at the weight ratios of 1:9, 2:8, 3:7, 4:6, 5:5, 6:4, 7:3, 8:2, and 9:1. NaCl solution (0.9%) was added drop by drop to each oily mixture under gentle magnetic stirring. The microemulsion systems were prepared using oleic acid as an oil phase, Cremophor EL as a surfactant, isopropanol as a co-surfactant and 0.9% NaCl solution as an aqueous phase. Finally, 2 mg of Aprotinin was labeled with ^{99m}Tc according to above studies and slowly incorporated into the 10 ml microemulsion as an aqueous phase under stirring and mixed the other composition of microemulsion. According to these diagrams, which have been created by means of a computer program (Ege et al., 2004), it was considered that the optimum microemulsion contained 9.34% oleic acid, 18% Cremophor EL, 36% isopropanol and 36.66% saline. The mixture was observed for transparency. ^{99m}Tc-Aprotinin-M was filtered through a 0.22-μm pore sized membrane sterile filter (Minisart, Sartorius) into a sterile vial under laminar airflow Class II cabinet (EsCo Class 2 ACIIG34M, Selangor, Malaysia).

Animal studies

Adult male Wistar albino rats (3–6 months age) weighing 250 ± 20 g were purchased from the Experimental Animal Center of Ege University (Izmir, Turkey) for the *in vivo* and histopathology studies. The experimental protocol was approved by the Local Animal Ethical Committee of Ege University, Faculty of Pharmacy (Approval No. E.U 1344–249). Rats were housed in a room maintained at $22 \pm 1\,^{\circ}C$ with an alternating 12 h light–dark cycle. Animals had free access to pellet diet and water *ad libitum*. The rats were transported to a quiet laboratory at least 1 h before the experiment began.

Induction of experimental mild acute pancreatitis model (with cerulein). Seven rats were randomly selected and used for induction of mild acute pancreatitis model. An experimental model of acute edematous pancreatitis was created with four subcutaneous injections of 20 μg/kg cerulein in every hour up to 4 h.

Induction of experimental severe acute pancreatitis model (with sodium taurocholate). Severe necrotizing pancreatitis was induced by intraductal (ID) infusion of 3% taurocholate. Under sterile conditions, a midline laparotomy was performed and the common biliopancreatic duct was cannulated with a 27-gauge needle. The seromuscular layer of duodenum was punctured 2–3 mm away from the entrance of biliary duct. The needle was introduced into the duct. The distal biliopancreatic duct ligated to avoid reflux of taurocholate into the duodenum. To prevent leakage of bile salt into the liver, the bile duct was clamped temporarily near the hepatic hilum. Sterile 3% sodium taurocholate (0.1 ml/100 g of body weight) or serum physiologic (SP) was infused slowly. After the infusion completed, the needle and the ligature were removed, the hepatic hilum was decamped and the abdominal wound was closed in two layers.

Induction of air pouch model. The air pouch was formed by initial s.c. injection of 20 ml air into back of male Wistar albino rats and injection of 10 ml air every 3 days to sustain its patency (Buluç et al., 2002). Six days after the initial injection of air, 2 ml of 1% carrageenan solution in sterile 0.9% NaCl was injected into the cavity. Six hours after carrageenan injection, the animals were anesthetized with ether and 1 ml of heparinized saline was given to wash out the cavity. The pouch cavity was opened and the exudate was harvest 6 h after injecting carrageenan.

Scintigraphic imaging studies of ^{99m}Tc-Aprotinin

After the acute edematous, severe necrotizing pancreatitis and air pouch model was induced gamma scintigraphy and bioavailability studies were performed.

Gamma scintigraphy and biodistribution studies were performed with acute edematous, severe necrotizing pancreatitis and air pouch model induced rats. For experiments rats, 0.1 mCi ^{99m}Tc-Aprotinin-S solution and ^{99m}Tc-Aprotinin-M was injected to the anesthetized rats via tail vein. During the scintigraphy studies animals were keep under anesthetize with ketamine/xylazin mixture. The scintigraphic images were obtained with a dual head gamma camera (Infinia General Electric) equipped with a low-energy high-resolution collimator viewing the whole body of rats. After administration of radiopharmaceuticals, serial static images were acquired in a 256×256 matrix for 60 s each, at different time intervals (5, 15, 30, 45, 60 and 90 min post-injection) up to 90 min.

Biodistribution studies

Ninety minutes after injection, the rats were sacrificed and biodistribution was determined. Samples of heart, liver, spleen, pancreas, lung, kidney and blood were weighed and the radioactivity was measured using a gamma counter (Sesa Uniscaller, Germany). The percentage of injected dose per gram of tissue (%ID/g) was calculated and the results were expressed as organ/blood ratios.

Statistical analysis

The calculation of means and standard deviations was performed on Microsoft Excel. One-way ANOVA was used to determine statistical significance. Differences at the 95% confidence level ($p < 0.05$) were considered significant. Experiments were performed in triplicate unless stated otherwise. Results are reported as mean ± standard error.

Results

Radiolabeling studies

Aprotinin was labeled with ^{99m}Tc by a direct labeling method. Labeling efficiency of the ^{99m}Tc-Aprotinin was assessed by

Table 1. Rf values of ^{99m}Tc-Aprotinin in mobile phases.

	Whatman 3MM	ITLC-SG[a]
	Acetone	A/E/W
Free ^{99m}Tc	0.7–1.0	0.7–1.0
R/H ^{99m}Tc	0.0	0.0
^{99m}Tc-Aprotinin	0.0	0.7-1.0

[a]Albumin impregnated.

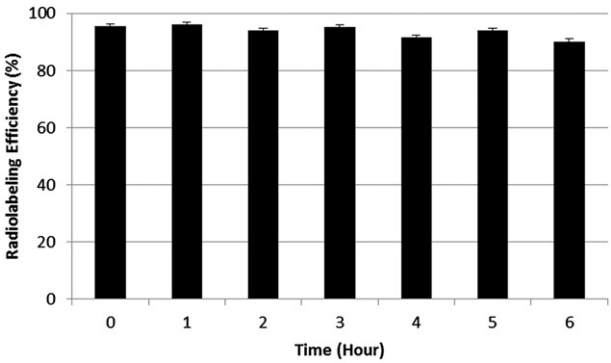

Figure 1. Radiolabeling efficiency and stability of ^{99m}Tc-Aprotinin at room temperature up to 6 h.

RTLC studies. Two solvent systems were used to distinguish and quantify the amounts of radioactive contaminants.

In RTLC, using acetone as the solvent, free ^{99m}Tc moved with the solvent front, while ^{99m}Tc-Aprotinin and R/H ^{99m}Tc remained at the spotting point. R/H ^{99m}Tc was determined by using A/E/W (1/2/5) as the mobile phase where the R/H ^{99m}Tc remained at the point of spotting, while free ^{99m}Tc and ^{99m}Tc-Aprotinin moved with the solvent front. The Rf values of ^{99m}Tc-Aprotinin in mobile phases are presented in Table 1.

According to our study Aprotinin was radiolabeled by ^{99m}Tc with high RP ($95.430 \pm 0.946\%$). The complex was found to be stable at room temperature up to 6 h without any significant changes of labeling yield ($p > 0.05$) (Figure 1).

Scintigraphic imaging studies of ^{99m}Tc-Aprotinin

The uptake of ^{99m}Tc-Aprotinin-S and ^{99m}Tc-Aprotinin-M following intravenous administrations was assessed on static images (Figures 2–4).

For quantitative evaluation, regions of interest were drawn around the liver, spleen and kidney of the rats. The ^{99m}Tc-Aprotinin uptake was calculated by dividing the average counts per pixel within the region of organs to the average counts per pixel within the region of background (Figures 5 and 6).

Biodistribution studies

Based on data presented in Tables 2–4, biodistribution of ^{99m}Tc-Aprotinin-S and ^{99m}Tc-Aprotinin-M was determined for heart, liver, pancreas, lung, spleen and kidney of acute edematous, severe necrotizing pancreatitis and air pouch model induced rats at 90 min after injection.

The biodistribution studies depicted that the ^{99m}Tc-Aprotinin-S and ^{99m}Tc-Aprotinin-M have different distribution speeds and regions throughout the body after injection.

Discussion

Previously, Aprotinin was radiolabeled with ^{99m}Tc and ^{131}I for different aimed studies (Bianchi et al., 1984; Aprile et al., 1986,1995; Rustom et al., 1992; Schaadt et al., 2003). Since ^{99m}Tc is one of the most popular radionuclide for gamma scintigraphy studies with its versatile chemistry, good photon energy (140 keV) and suitable half-life (6 h), in this study ^{99m}Tc was chosen as the radionuclide to label Aprotinin (Aprile et al., 1986,1995).

Different types of reducing agents were used to reduce ^{99m}Tc from the +7 oxidation state to more reactive +5 oxidation state to promote binding. Smyth and Tsopelas were prefer to use stannous pyrophosphate (PYP) as a reducing agent in ready to use kit formulation and the authors conclude that the PYP played an important role in stabilizing stannous and reduced technetium in the alkaline environment of the cold kit (Smyth & Tsopelas, 2005). The cold kits proved to be stable to long-term storage for up to 6 months, and the radiotracer was stable for at least 4 h. In this study, stannous chloride was used as a reducing agent and the complex was found to be stable at room temperature up to 6 h with the labeling efficiency >90%.

Han et al. was prepared ^{99m}Tc-Aprotinin by using freshly prepared stannous chloride solution in acidic media. The authors found the RP of the complex immediately after preparation >95% as well as our experiments. So, our results are found to be in compliance with the results of the reference method (Han et al., 2007).

Animal studies have shown that similar to that of other small proteins Aprotinin is accumulated primarily in the kidney. Aprotinin, after being filtered by the glomeruli, is actively reabsorbed by the proximal tubules in which it is stored in phagolysosomes. Aprotinin is slowly degraded by lysosomal enzymes. Following a single i.v. dose of radiolabeled Aprotinin, approximately 25–40% of the radioactivity is excreted in the urine >48 h (FDA, http://www.fda.gov/downloads/Drugs/DrugSafety/PostmarketDrugSafetyInformationforPatientsandProviders/UCM142741.pdf). Our results indicate that for both ^{99m}Tc-Aprotinin-S and ^{99m}Tc-Aprotinin-M the highest radioactivity was observed in kidneys. This result suggests that the ^{99m}Tc-Aprotinin was removed from the circulation mainly through the kidneys and urine, which is compatible with the elimination route of the cold Aprotinin.

Since site and route of administration impact biodistribution of pharmaceuticals, the tissue distribution profiles of ^{99m}Tc-Aprotinin-S and ^{99m}Tc-Aprotinin-M group were compared in rats. The concentration of Aprotinin in each tissue was determined by a gamma counter. As shown in Tables 2–4, Aprotinin was distributed into most tissues following intravenous administration. While the highest concentration of Aprotinin was found in kidney for both formulations, kidney/blood (%ID/g) ratios show a significant higher uptake ratio of Aprotinin after ^{99m}Tc-Aprotinin-S injection ($p < 0.05$) than ^{99m}Tc-Aprotinin-M. This result indicates that the newly developed microemulsion formulation was change the distribution of Aprotinin after i.v. injection.

Many studies have demonstrated that nanoformulations show significant difference in pharmacological and

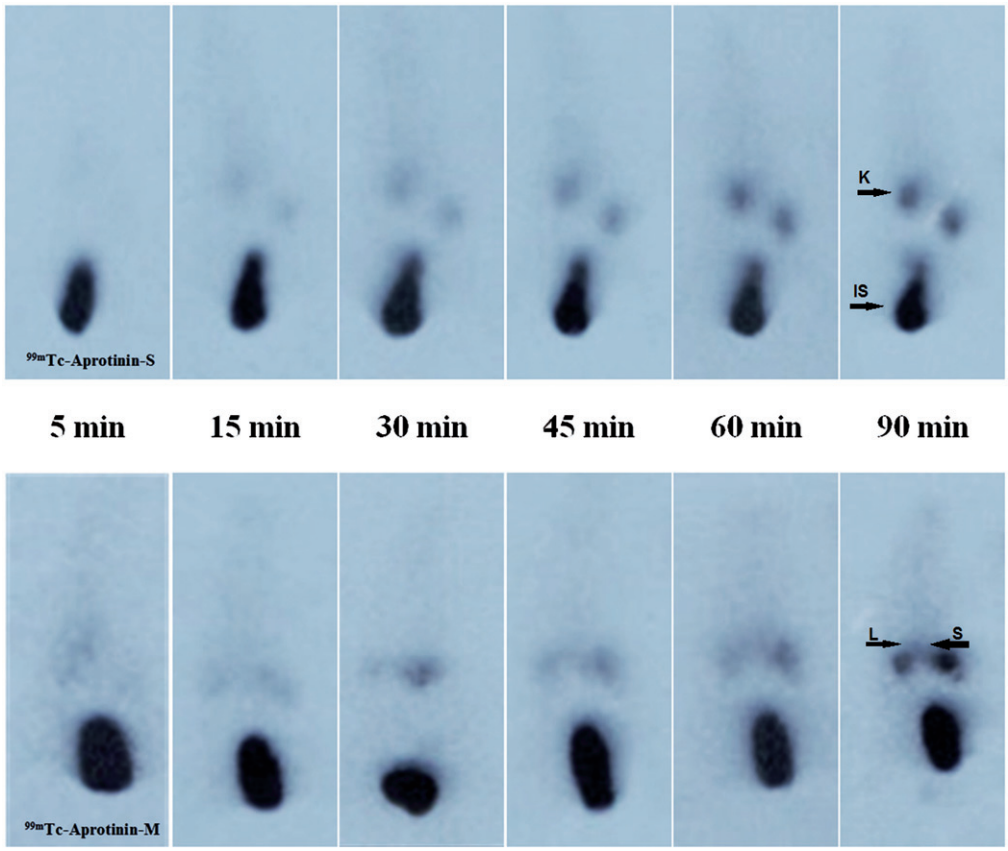

Figure 2. The scintigrams of ^{99m}Tc-Aprotinin-S and ^{99m}Tc-Aprotinin-M injected acute edematous, model induced rats at different time intervals up to 90 min (approximate organ regions for K: kidney, IS: injection site, L: liver, S: spleen).

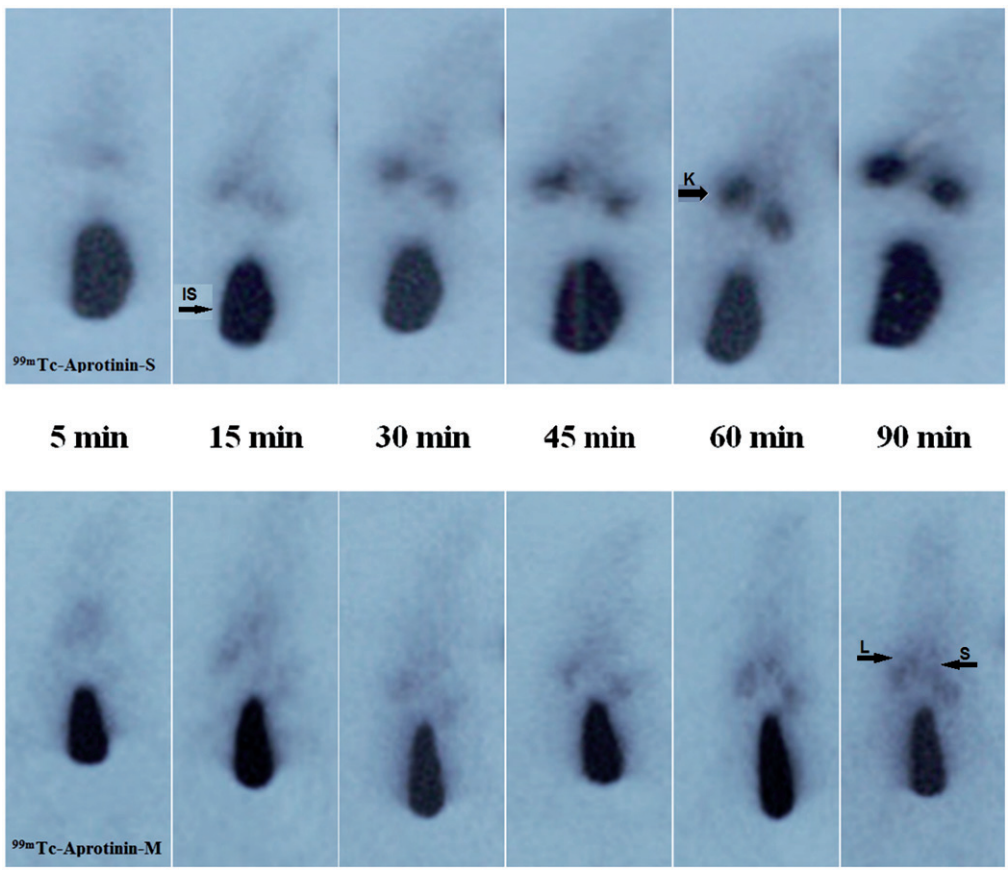

Figure 3. The scintigrams of ^{99m}Tc-Aprotinin-S and ^{99m}Tc-Aprotinin-M injected severe necrotizing pancreatitis model induced rats at different time intervals up to 90 min (approximate organ regions for K: kidney, IS: injection site, L: liver, S: spleen).

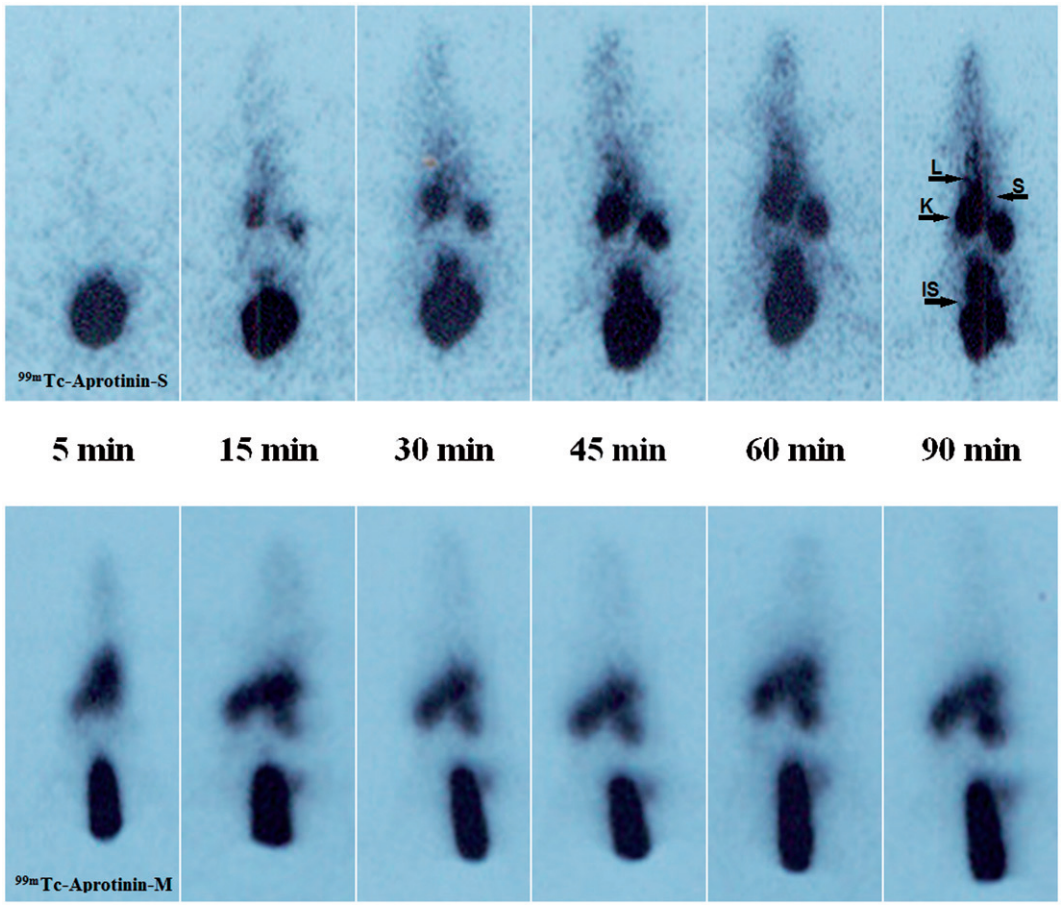

Figure 4. The scintigrams of ^{99m}Tc-Aprotinin-S and ^{99m}Tc-Aprotinin-M injected air pouch model induced rats at different time intervals up to 90 min (approximate organ regions for K: kidney, IS: injection site, L: liver, S: spleen).

Figure 5. Calculated Organ/BG ratios of acute edematous (A), severe necrotizing pancreatitis (B) and air pouch model (C) induced rats after ^{99m}Tc-Aprotinin-S injection up to 90 min.

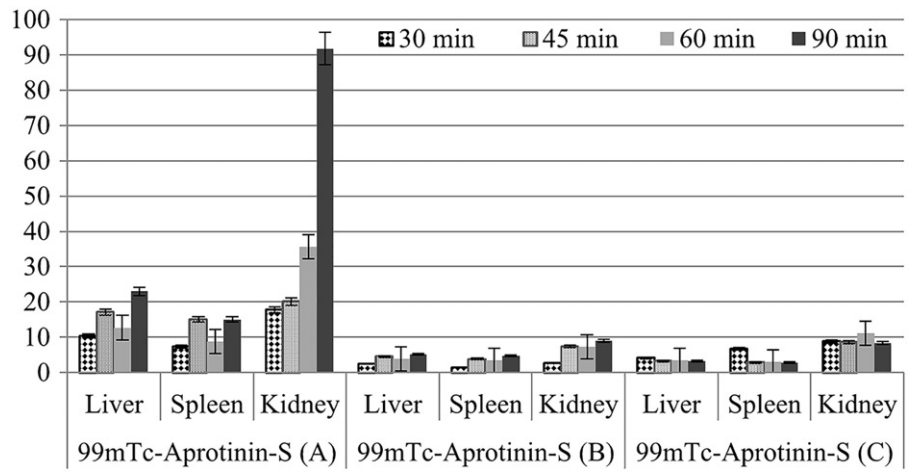

toxicological properties, such as organ targeting, increased efficacy, reduced toxicity, from bulk material of the same composition due to their nanoscale size (Gabizon et al., 2006; Ellis-Behnke et al., 2007; Kim, 2007). Whereas the larger micelles with the size range of 50–100 nm were removed by the liver and spleen, polymeric micelles smaller than 5 and 5–10 nm were easily eliminated through the renal glomeruli (Kedar et al., 2010). According to our previously published study about formulation, characterization, biodistribution and therapeutic potential of new Aprotinin microemulsion in acute pancreatitis the average droplet size was found 64.55 ± 3.217 nm for Aprotinin microemulsion formulation (Karasulu et al., 2015). As it was expected, the results of the scintigraphy and biodistribution studies showed that, while i.v. administration of ^{99m}Tc-Aprotinin-S distributed mostly in kidneys and bladder, ^{99m}Tc-Aprotinin-M, with droplet size of 64.550 ± 3.217 nm, has high uptake in liver and spleen.

In addition to the above information, this theoretical information does not always give the same result practically. As an illustration the authors were prepared a novel paclitaxel

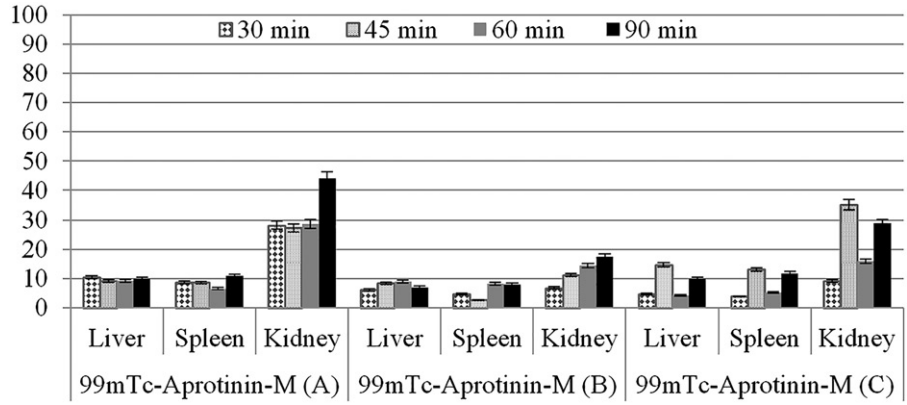

Figure 6. Calculated organ/BG ratios of acute edematous (A), severe necrotizing pancreatitis (B) and air pouch model (C) induced rats after ^{99m}Tc-Aprotinin-M injection up to 90 min.

Table 2. Biodistribution results of (organ/blood ratios) ^{99m}Tc-Aprotinin-S and ^{99m}Tc-Aprotinin-M injected acute edematous (A) induced rats at 90 min post-injection.

	Organ/blood uptake ratios	
	^{99m}Tc-Aprotinin-S	^{99m}Tc-Aprotinin-M
Heart	0.407 ± 0.033	0.494 ± 0.106
Liver	0.847 ± 0.108	1.160 ± 0.012
Pancreas	0.752 ± 0.060	1.269 ± 0.018
Lung	0.612 ± 0.504	0.689 ± 0.008
Spleen	0.496 ± 0.019	0.520 ± 0.011
Kidney	9.484 ± 4.626	1.372 ± 0.764

microemulsion and compare the pharmacokinetics, biodistribution, *in vivo* antitumor activity and safety results of paclitaxel microemulsion with solution. According to the study, the author concludes that there was no significant difference in the tissue distribution of paclitaxel between the paclitaxel microemulsion group and the paclitaxel injection group (Ying et al., 2011).

Table 3. Biodistribution results of (organ/blood ratios) ^{99m}Tc-Aprotinin-S and ^{99m}Tc-Aprotinin-M injected severe necrotizing pancreatitis (B) induced rats at 90 min post-injection.

	Organ/blood uptake ratios	
	^{99m}Tc-Aprotinin-S	^{99m}Tc-Aprotinin-M
Heart	0.438 ± 0.024	0.652 ± 0.047
Liver	0.976 ± 0.199	2.000 ± 0.016
Pancreas	0.472 ± 0.031	1.435 ± 0.013
Lung	0.899 ± 0.047	0.565 ± 0.007
Spleen	0.325 ± 0.026	0.826 ± 0.011
Kidney	2.662 ± 1.913	1.439 ± 0.719

Table 4. Biodistribution results of (organ/blood ratios) ^{99m}Tc-Aprotinin-S and ^{99m}Tc-Aprotinin-M injected air pouch model (C) induced rats at 90 min post-injection.

	Organ/blood uptake ratios	
	^{99m}Tc-Aprotinin-S	^{99m}Tc-Aprotinin-M
Heart	0.483 ± 0.056	0.473 ± 0.011
Liver	0.814 ± 0.022	0.464 ± 0.011
Pancreas	0.331 ± 0.018	0.328 ± 0.144
Lung	0.246 ± 0.014	1.693 ± 0.019
Spleen	0.314 ± 0.060	0.579 ± 0.230
Kidney	7.58 ± 2.965	1.6740 ± 0.485

In this study, air pouch model was created to investigate whether ^{99m}Tc-Aprotinin-M was uptake by sham inflammation or pancreas. liver/blood and pancreas/blood uptake ratios for acute edematous and severe necrotizing pancreatitis model induced rats after ^{99m}Tc-Aprotinin-M injection was found to be higher than air pouch model induced rats. This might be concluding that microemulsions may be suggested as promising formulations for selectively targeting Aprotinin to pancreas inflammation. Also, according to our previously published work results about intravenous administration of developed Aprotinin loaded microemulsion the Aprotinin loaded microemulsion does not lead any pancreatic damage itself so it may be considered as safe (Karasulu et al., 2015).

When %ID/g per organ evaluated (data not shown) the counted radioactivity of severe pancreatitis model induced rats' organs was found lower than acute pancreatitis models induced rats. This slower biodistribution of both the formulations in that model might be explained with the failure circulatory and fluid loss after Taurocholate-induced pancreatitis model induction.

Conclusion

Aprotinin is theoretically attractive molecule in ameliorating the effects of acute pancreatitis (Bjerregaard et al., 2001; Smith et al., 2009). Over the following two decades Aprotinin therapeutic potential on pancreatitis is proven experimentally but its clinical therapeutic success is limited due to low targeting to pancreas. In our previously published work, Aprotinin microemulsion was developed, characterized and therapeutic potential in acute pancreatitis was evaluated (Karasulu et al., 2015).

The aim of this study was to evaluate the biodistribution of ^{99m}Tc-Aprotinin-S and ^{99m}Tc-Aprotinin loaded microemulsion which was prepared for the aim of the treatment for acute pancreatitis.

^{99m}Tc-Aprotinin was prepared using previously published method (Han et al., 2007). Labeling efficiency of ^{99m}Tc-Aprotinin was assessed by RTLC and found higher than 90%. The resulting complex was quite stable and labeling of >90% was maintained for up to 6 h. After observing the optimum labeling conditions for maximum labeling efficiency and stability, ^{99m}Tc-Aprotinin loaded to the microemulsion

formulation and *in vivo* gamma scintigraphy and biodistribution studies were performed with acute edematous, severe necrotizing pancreatitis and air pouch model induced rats.

According to the gamma scintigraphy studies, ^{99m}Tc-Aprotinin-S and ^{99m}Tc-Aprotinin-M have different distribution speeds and regions throughout the body after injection. The biodistribution studies depicted that, while ^{99m}Tc-Aprotinin-S distributed mostly in kidneys and bladder, ^{99m}Tc-Aprotinin-M has high uptake in liver and spleen. Also, liver/blood and pancreas/blood uptake ratios for acute edematous and severe necrotizing pancreatitis model induced rats after ^{99m}Tc-Aprotinin-M injection was found to be higher than air pouch model induced rats.

Collectively, these results indicate that the microemulsions may be suggested as promising formulations for selectively targeting Aprotinin to pancreas inflammation.

Acknowledgements

The authors would like to thank Caglar Us, Ismail Zonguldak, Bulent Ata and Ege University Nuclear Medicine Department technicians for their technical assistance for the animal experiments. Also, the authors would like to thank Ege University Nuclear Medicine Department for their support to supply the radionuclide.

Declaration of interest

The authors declare no conflict of interest. The authors alone are responsible for the content and writing of the article. This study was supported by The Scientific and Technological Research Council of Turkey (Tübitak 108S083). The authors also thank to the T.R. Prime Ministry State Planning Organization Foundation (Project Number: 09DPT001).

References

Ajit SN, David D, Danchen G. (2007). Stable drug encapsulation in micelles and microemulsions. Int J Pharm 345:9–25.

Aprile C, Marinone G, Saponaro R, et al. (1995). Cardiac and pleuropulmonary AL amyloid imaging with technetium-99m labelled aprotinin. Eur J Nucl Med 22:1393–401.

Aprile C, Saponaro R, Villa G, et al. (1986). Assessment of split renal function with ^{99m}Tc-aprotinin. Eur J Nucl Med 12:37–40.

Bianchi C, Donadio C, Tramonti G, et al. (1984). ^{99m}Tc Aprotinin: a new tracer for kidney morphology and function. Eur J Nucl Med 9:257–60.

Bjerregaard S, Andersen LW, Stephens RW, et al. (2001). Sustained elevated plasma aprotinin concentration in mice following intraperitoneal injections of w/o emulsions incorporating aprotinin. J Control Release 71:87–98.

Bode W, Huber R. (1992). Natural protein proteinase inhibitors and their interaction with proteinases. Eur J Biochem 204:433–51.

Buluç M, Gürdal H, Melli M. (2002). Effect of misoprostol and indomethacin on cyclooxygenase induction and eicosanoid production in carrageenan-induced air pouch inflammation in rats. Prostaglandins Other Lipid Mediat 70:227–39.

Burke MD, Staton JS, Viskers AW, et al. (2007). A novel method to radiolabel gastric retentive formulations for gamma scintigraphy assessment. Pharm Res 24:695–704.

Edward LA. (1993). Clinically Based classification system for acute pancreatitis: summary of the International Symposium on Acute Pancreatitis, Atlanta, GA, September 11 through 13, 1992. Arch Surg 128:586–90.

Ege MA, Karasulu HY, Guneri T. (2004). Triangle phase diagram analysis software. Presented at: The 4th International Postgraduate Research Symposium on Pharmaceutics, Istanbul, Turkey. 46, 36.

Ellis-Behnke R, Teather L, Schneider G, So K. (2007). Using nanotechnology to design potential therapies for CNS regeneration. Curr Pharm Des Pharm 13:2519–28.

Gabizon AA, Tzemach D, Horowitz AT, et al. (2006). Reduced toxicity and superior therapeutic activity of a mitomycin C lipid-based prodrug incorporated in pegylated liposomes. Clin Cancer Res 12: 1913–20.

Graf A, Ablinger E, Peters S, et al. (2008). Microemulsions containing lecithin and sugar-based surfactants: nanoparticle templates for delivery of proteins and peptides. Int J Pharm 350:351–60.

Häfeli U. (2002). Radioactive microspheres for medical applications. In: De Cuyper M, Bulte JWM, eds. Physics and chemistry basis of biotechnology. Kluwer Academic Publishers, Springer Netherlands, 213–48.

Han S, Chong V, Murray T, et al. (2007). Preliminary experience of ^{99m}Tc-Aprotinin scintigraphy in amyloidosis. Eur J Haematol 79: 494–500.

Henry DA, Carless PA, Moxey AJ, et al. (2011). Anti-fibrinolytic use for minimising perioperative allogeneic blood transfusion. Cochrane Database Syst Rev CD001886. doi: 10.1002/14651858. CD001886.pub3.

Hunt BJ, Segal H, Yacoub M. (1992). Aprotinin and heparin monitoring during cardiopulmonary bypass. Circulation 86:410–12.

Kalkat M, Levine A, Dunning J. (2004). Does use of aprotinin in coronary artery bypass graft surgery affect graft patency? Interact Cardiovasc Thorac Surg 3:124–8.

Karasulu HY, Oruç N, Üstündağ-Okur N, et al. (2015). Aprotinin revisited: formulation, characterization, biodistribution and therapeutic potential of new aprotinin microemulsion in acute pancreatitis. J Drug Target 23:525–37.

Kedar U, Phutane P, Shidhaye S, Kadam V. (2010). Advances in polymeric micelles for drug delivery and tumor targeting. – Nanomedicine Nanotechnol 6:714–29.

Kim K. (2007). Nanotechnology platforms and physiological challenges for cancer therapeutics. Nanomedicine 3:103–10.

Krauser JA. (2013). A perspective on tritium versus carbon-14: ensuring optimal label selection in pharmaceutical research and development. J Labelled Comp Radiopharm 56:441–6.

Park K. (2007). Nanotechnology: what it can do for drug delivery. J Control Release 120:1–3.

Rustom R, Grime S, Maltby P, et al. (1992). A new method to measure renal tubular degradation of small filtered proteins in man using radiolabelled aprotinin (Trasylol). Clin Sci 83:289–94.

Schaadt BK, Hendel HW, Gimsing P, et al. (2003). ^{99m}Tc-aprotinin scintigraphy in amyloidosis. J Nucl Med 44:177–83.

Smith M, Kocher HM, Hunt BJ. (2009). Aprotinin in severe acute pancreatitis. Int J Clin Pract 64:84–92.

Smyth DR, Tsopelas C. (2005). An improved (99m)Tc-aprotinin kit formulation: quality control analysis of radiotracer stability and cold kit shelf life. Nucl Med Biol 32:885–9.

Tiourina O, Sharf T, Balkina A, et al. (2003). Interaction of the water-soluble protein aprotinin with liposomes: gel-filtration, turbidity studies, and 31P NMR studies. J Liposome Res 13:213–29.

Üstündağ-Okur N, İlem-Özdemir D, Görgülü Kahyaoğlu Ş, et al. (2015). Assessment of aprotinin loaded microemulsion formulations for parenteral drug delivery: preparation, characterization, *in vitro* release and cytotoxicity studies. Curr Drug Deliv 12:668–79.

Wilding IR, Coupe AJ, Davis SS. (1991). The role of gamma scintigraphy in oral drug delivery. Adv Drug Deliv Rev 7:87–117.

Ying W, Ke-Chun W, Bing-Xiang Z, et al. (2011). A novel paclitaxel microemulsion containing a reduced amount of Cremophor EL: pharmacokinetics, biodistribution, and *in vivo* antitumor efficacy and safety. J Biomed Biotechnol 2011:854872. doi: 10.1155/2011/854872.